

Stability and dynamics of anisotropically-tumbling chemotactic swimmers

Enkeleida Lushi¹

¹*School of Engineering, Brown University, Providence RI 02912, USA^a*

(Dated: March 10, 2016)

Micro-swimmers such as bacteria are known to perform random walks known as run-and-tumbles to move up chemo-attractant gradients and as a result aggregate. It is also known that such micro-swimmers can self-organize into macroscopic patterns due to interactions with neighboring cells through the fluidic environment they live in. While the pattern formation resulting from chemotactic and hydrodynamic interactions separately and together have been previously investigated, the effect of the tumbling anisotropy in micro-swimmers has been unexplored. Here we show through linear analysis and full nonlinear simulations that the slight anisotropy in the individual swimmer tumbles can alter the collective pattern formation in non-trivial ways. We show that the tumbling anisotropy diminishes the magnitude of the chemotactic aggregates but may result in more such aggregation peaks.

PACS numbers: 87.17.Jj, 05.20.Dd, 47.63.Gd, 87.18.Hf

Keywords: chemotaxis, locomotion, cell motility, hydrodynamics, kinetic theory, microorganisms, suspensions

I. INTRODUCTION

Micro-swimmers such as bacteria *Escherichia coli* perform a biased random walk that enables them to move up regions of increasing chemical they are attracted to⁴. This chemo-attractant is typically food they consume, but can also be chemicals that bacteria signal each-other with² in quorum sensing and communication²⁰. The random walk bacteria perform, consisting of a sequence of straight runs and tumbles, is biased as the mean run duration increases when a bacterium moves in the direction of the chemo-attractant gradient. As a result, the bacteria eventually aggregate in regions of high chemo-attractant levels. Though for simplicity most mathematical models studying chemotaxis and bacterial random walks assume independence of the pre- and post-tumble directions, in bacteria like *E. coli* these directions are in fact correlated^{25,28}. This slight correlation in tumbles can result in a different individual and collective dynamics that has not been explored much.

Many motile bacteria live in fluidic environments and their mechanical interactions through this medium can affect their collective self-organization even in the absence of externally-imposed flows, chemical cues or other possible stimuli^{8,10}. If the bacteria are chemotactic, the chemicals they produce or consume can be transported or diffused in the fluid, and hence the modes of communication as well as pattern formation can be affected. In particular, micro-swimmers like bacteria, which propel using rear-mounted flagella and are classified as *pushers*, are known to self-organize in structures larger in scale and speed than an individual due to direct and hydrodynamical interactions^{8,10,23,27,29}. In a recent study¹⁶, we found that fully coupling the fluid motion to the dynamics of the swimmers and chemo-attractant can greatly affect and modify the colony's pattern formation.

Here we explore the combined effects of the anisotropic chemotaxis and the collectively-generated fluid flows through linear analysis and nonlinear simulations. The Run-and-Tumble chemotaxis model we use here is based on Alt's work¹, and subsequent analysis of Schnitzer²⁵, Bearon and Pedley³, and Chen *et. al.*⁷ on a continuum formulation of the biased random walk in three dimensions. In particular, we extend our recent model of chemotactic dynamics in the presence of self-generated fluid flows^{16,17} to include an anisotropic run-and-tumble chemotactic response in the theory of motile suspensions.

We discover that while the major changes in the chemotactic pattern formation happens due to the collectively-generated fluid flows, the anisotropy in the tumbles results in subtle but non-trivial alterations. Linear analysis predicts that the tumbling anisotropy can stabilize the concentration growth due to chemotaxis, though it has little effect on the instability due to hydrodynamic interactions between the swimmers. Full nonlinear simulations of the coupled equations reveal that not only does the tumble anisotropy subsid the chemotactic aggregation, it generally results in more aggregation peaks that are lower in magnitude.

II. MATHEMATICAL MODEL

A. Run-and-Tumble Auto-Chemotaxis in 3D

We consider ellipsoidal swimmers moving with an intrinsic speed $U_0 := 1$ in a 3D fluid domain. A swimmer's center of mass is denoted by \mathbf{x} and its swimming direction \mathbf{p} (with $\mathbf{p} \cdot \mathbf{p} = 1$) is along the main axis. The configuration of micro-swimmers is given by the distribution function $\Psi(\mathbf{x}, \mathbf{p}, t)$. The dynamics of a colony of swimmers that each do run-and-tumble biased walks, can be

^a)Electronic mail: enkeleida.lushi@brown.edu

described by a Fokker-Planck conservation equation

$$\frac{\partial \Psi}{\partial t} = -\nabla_x \cdot [\Psi \dot{\mathbf{x}}] - \nabla_p \cdot [\Psi \dot{\mathbf{p}}] - [\Psi \lambda(\mathcal{D}_t C) - \int \mathbf{K}(\mathbf{p}, \mathbf{p}'; \delta) \Psi(\mathbf{p}') \lambda(\mathcal{D}_t C) d\mathbf{p}'] \quad (1)$$

$$\dot{\mathbf{x}} = U_0 \mathbf{p} + \mathbf{u} - D \nabla_x (\ln \Psi) \quad (2)$$

$$\dot{\mathbf{p}} = (\mathbf{I} - \mathbf{p}\mathbf{p})(\gamma \mathbf{E} + \mathbf{W})\mathbf{p} - d_r \nabla_p (\ln \Psi). \quad (3)$$

Equations (2) and (3) refer to fluxes associated with the swimmer position and orientation. Equation (2) describes a swimmer propelling along its main axis \mathbf{p} with constant speed U_0 while also being advected by the background fluid flow \mathbf{u} . The last term in the flux describes isotropic translational diffusion with constant D . Equation (3) describes the rotation of an ellipsoid by the local fluid flow, with $\mathbf{E} = (\nabla \mathbf{u} + \nabla^T \mathbf{u})/2$, $\mathbf{W} = (\nabla \mathbf{u} - \nabla^T \mathbf{u})/2$ being the rate-of-strain and vorticity tensors, respectively, and γ a shape parameter $-1 \leq \gamma \leq 1$ (for a sphere $\gamma = 0$ and for an elongated particle $\gamma \approx 1$). The last term in Eq. (3) models rotational diffusion of the swimmer with constant d_r , as done in^{17,24}.

The run-and-tumble chemotaxis is described by the terms in the bracket in Eq. (1). The first term describes the loss of swimmers tumbling from orientation \mathbf{p} to other orientations, and the second term accounts for swimmers tumbling to \mathbf{p} from other orientations \mathbf{p}' . As in Alt's work and consequent models^{1,7,25}, runs are assumed straight and the tumbles instantaneous. Here $\lambda(\mathcal{D}_t C)$ is tumbling frequency or stopping rate, and is related to the probability of a bacterium tumbling over a finite time interval. From experiments¹⁸ it is known that when the time rate of change of the chemo-attractant gradient is positive along a swimmer's path, the swimmer's tumbling frequency reduces. If the chemo-attractant concentration is constant or decreasing, the stopping rate remains constant. Based on experimental data¹⁸ and theoretical studies⁷, this biphasic response for $\lambda(\mathcal{D}_t C)$ can modeled as

$$\lambda(\mathcal{D}_t C) = \begin{cases} \lambda_0 \exp(-\chi \mathcal{D}_t C) & \text{if } \mathcal{D}_t C > 0 \\ \lambda_0 & \text{otherwise,} \end{cases} \quad (4)$$

where

$$\mathcal{D}_t C = \frac{\partial C}{\partial t} + (\mathbf{u} + U_0 \mathbf{p}) \cdot \nabla C \quad (5)$$

is the rate-of-change of the chemo-attractant concentration along the swimmer's path. The parameter λ_0 is the basal tumbling frequency or stopping rate in the absence of chemotaxis, χ the chemotactic strength or sensitivity. In literature the chemotactic response has been modeled in various forms, e.g. exponential as above⁷, linearized³, but usually does not include the temporal gradient, the swimmer propulsion or its advection by the fluid³⁰. Our recent work^{16,17} includes both the chemo-attractant and fluid dynamics.

We include the tumbling frequency $\lambda(\mathcal{D}_t C)$ in a piecewise linearized form of Eq. (4)

$$\lambda(\mathcal{D}_t C) = \begin{cases} \lambda_0 (1 - \chi \mathcal{D}_t C) & \text{if } 0 < \mathcal{D}_t C < 1/\chi \\ 0 & \text{if } 1/\chi < \mathcal{D}_t C \\ \lambda_0 & \text{otherwise} \end{cases}$$

Here the integral term in Eq. (1) includes a "turning kernel" $\mathbf{K}(\mathbf{p}, \mathbf{p}'; \delta)$ which represents a conditional probability of a bacterium tumbling from direction \mathbf{p} to post-tumble direction \mathbf{p}' . The parameter δ represents a correlation of the pre- and post-tumble directions, motivated by the fact that the tumbles are not perfectly random even in the absence of chemotaxis. Mathematically, the anisotropy is dependent on the absolute difference $|\mathbf{p} - \mathbf{p}'|$. A natural choice for the turning kernel dependent on this different is then an exponential form $\exp(\delta(\mathbf{p} \cdot \mathbf{p}'))$. The turning kernel has to satisfy a few conditions^{25,28}, namely:

- The integral over all directions should equal 1, thus $\int d\mathbf{p} \mathbf{K}(\mathbf{p}, \mathbf{p}'; \delta) = 1$, as the number of swimmers is conserved.
- $\mathbf{K}(\mathbf{p}, \mathbf{p}'; \delta) \rightarrow 1/4\pi$ as $\delta \rightarrow 0$, so the tumbles should be perfectly isotropic in the case of no correlations between pre- and post-tumble directions.
- $\mathbf{K}(\mathbf{p}, \mathbf{p}'; \delta) \rightarrow 0$ as $\delta \rightarrow \infty$, so each tumble leads to no changes.

Such a kernel is proposed by Subramanian and Koch²⁸

$$\mathbf{K}(\mathbf{p}, \mathbf{p}'; \delta) = \frac{\delta}{4\pi \sinh(\delta)} e^{\delta \mathbf{p} \cdot \mathbf{p}'}. \quad (6)$$

For $\delta \rightarrow 0$ we get perfectly isotropic tumbles while in the limit $\delta \rightarrow \infty$ each tumble leads to only infinitesimally small changes in direction, so we get "smoothly-turning swimmers". For *E. Coli*, $\delta \approx 1$, as also explained by²⁸, since their mean angle of tumbling is about 68° . Some previous studies, e.g.^{3,16,17}, have considered only isotropic tumbles, that is $\delta = 0$ and $\mathbf{K}(\mathbf{p}, \mathbf{p}'; 0) = 1/4\pi$. We will examine here the effects of this tumbling anisotropy in the dynamics of the active suspension, whether the swimmers in it are chemotactic or not.

The fluid velocity $\mathbf{u}(\mathbf{x}, t)$ satisfies the Stokes equations with an active stress due to the motile particles

$$-\nabla_x^2 \mathbf{u} + \nabla_x q = \nabla_x \cdot \Sigma^a \\ \nabla_x \cdot \mathbf{u} = 0. \quad (7)$$

Here μ is the viscosity of the surrounding fluid, q the fluid pressure, Σ^a the active stress

$$\Sigma^a(\mathbf{x}, t) = \alpha \int \Psi(\mathbf{x}, \mathbf{p}, t) (\mathbf{p}\mathbf{p}^T - \mathbf{I}/3) d\mathbf{p}. \quad (8)$$

The active stress is a configuration average over all orientations \mathbf{p} of the stresslets $\alpha(\mathbf{p}\mathbf{p}^T - \mathbf{I}/3)$ exerted by the

swimmers on the fluid^{23,28}. The stresslet strength α is a $O(1)$ constant that depends on the motility mechanism and swimmer geometry²⁴. For *pushers*, swimmers that propel themselves with rear-mounted flagella like bacteria *B. subtilis* or *E. coli*, $\alpha < 0$. For *pullers*, swimmers that propel themselves using front-mounted flagella like algae *C. Reinhardtii*, $\alpha > 0$.

We define a local swimmer concentration $\Phi(\mathbf{x}, t)$ as

$$\Phi(\mathbf{x}, t) = \int \Psi(\mathbf{x}, \mathbf{p}, t) d\mathbf{p}. \quad (9)$$

The chemo-attractant is dispersed in the fluid and has its own dynamics that includes fluid advection and diffusion. We model this similarly to the classical Keller-Segel model¹⁴ but here we include advection by fluid advection

$$\frac{\partial C}{\partial t} = -\mathbf{u} \cdot \nabla C - \beta_1 C + \beta_2 \Phi + D_c \nabla^2 C. \quad (10)$$

Here $-\beta_1 C$ describes chemo-attractant degradation with constant rate β_1 , and $\beta_2 \Phi$ describes the local production ($\beta_2 > 0$) of the chemo-attractant by the microswimmers themselves. The last term in Eq. (10) describes diffusion with coefficient D_c . Here we consider only *auto-chemotaxis* with $\beta_2 > 0$ where the chemo-attractant is produced by the swimmers themselves and not supplied externally.

The equation for the probability distribution function Ψ in Eq.(1), the chemo-attractant equation Eq.(10), together with the fluid equations Eq.(7), constitute a closed system describing the dynamics of a motile suspension influenced by an anisotropic run-and-tumble chemotaxis in an evolving chemical field.

For the anisotropic run-and-tumble autochemotaxis model in two dimensions, see the Appendix-VIA.

III. LINEAR STABILITY ANALYSIS

A. The Eigenvalue Problem

We analyze the linear stability of auto-chemotactic suspensions, $\beta_1, \beta_2 > 0$ in Eq. (10), about the uniform and isotropic state $\Psi_0 = 1/4\pi$. For simplicity, we consider no swimmer diffusion ($D = D_r = 0$) and only a quasi-static chemo-attractant field

$$-\beta_1 C + \beta_2 \Phi + D_c \nabla_x^2 C = 0. \quad (11)$$

We consider plane-wave perturbations of the distribution and chemo-attractant concentration functions about the uniform isotropic state ($\Psi_0 = 1/4\pi$) and steady-state ($\bar{C} = \beta_2/\beta_1$) respectively

$$\begin{aligned} \Psi(\mathbf{x}, \mathbf{p}, t) &= 1/4\pi + \epsilon \tilde{\Psi}(\mathbf{p}, \mathbf{k}) \exp(i\mathbf{k} \cdot \mathbf{x} + \sigma t) \\ C(\mathbf{x}, t) &= \beta_1/\beta_2 + \epsilon \tilde{C}(\mathbf{k}) \exp(i\mathbf{k} \cdot \mathbf{x} + \sigma t) \end{aligned}$$

with $|\epsilon| \ll 1$, \mathbf{k} the wavenumber and σ the growth rate.

This choice simplifies the stopping rate expression to

$$\lambda(\mathcal{D}_t C) = \lambda_0 (1 - \chi \mathbf{p} \cdot \nabla C). \quad (12)$$

When anisotropic tumbles are included in the chemotaxis model, the turning kernel $\mathbf{K}(\mathbf{p}, \mathbf{p}'; \delta)$ couples all the rotational moments and makes it difficult to analyze the problem. To get some insight on the role of anisotropy, we look at the linearized turning kernel for a small correlation parameter $\delta < 1$, which gives

$$K(\mathbf{p}, \mathbf{p}'; \delta) \approx \frac{1}{4\pi} + \frac{1}{4\pi} \delta \mathbf{p} \cdot \mathbf{p}'.$$

Substituting these into the linearized Eq. (1) we obtain

$$\begin{aligned} \frac{\partial \Psi}{\partial t} &= -\mathbf{p} \cdot \nabla \Psi + \frac{3\gamma}{4\pi} \mathbf{p} \mathbf{p} : \mathbf{E} \\ &- \lambda_0 \Psi + \frac{\lambda_0 \chi}{4\pi} \mathbf{p}^T \nabla C + \frac{\lambda_0}{4\pi} \int \Psi' d\mathbf{p}' \\ &+ \frac{\lambda_0 \delta}{4\pi} \mathbf{p}^T \int \Psi' \mathbf{p}' d\mathbf{p}' - \frac{\lambda_0 \delta}{4\pi} \frac{\chi}{4\pi} \mathbf{p}^T \int \Psi' \mathbf{p}' \mathbf{p}'^T d\mathbf{p}' \nabla C. \end{aligned} \quad (13)$$

Note that for the quasi-static form of the chemo-attractant above, the chemo-attractant field is tied to the dynamics of the swimmer concentration Φ , which is obtained from Ψ . We can then solve for \tilde{C} in terms of $\tilde{\Psi}$

$$\tilde{C} = \frac{\beta_2}{\beta_1 + k^2 D_c} \tilde{\Phi} = \frac{\beta_2}{\beta_1 + k^2 D_c} \int \tilde{\Psi}' d\mathbf{p}' \quad (14)$$

where $k = |\mathbf{k}|$. We can solve the fluid equations for the fluid velocity perturbation in terms of the active stress

$$\tilde{\mathbf{u}} = \frac{i}{k} (\mathbf{I} - \hat{\mathbf{k}} \hat{\mathbf{k}}^T) \cdot \tilde{\Sigma}^a \cdot \hat{\mathbf{k}} \quad (15)$$

with $\mathbf{k} = k \hat{\mathbf{k}}$. Since $\tilde{\Sigma}^a = \alpha \int \tilde{\Psi}' \mathbf{p}' \mathbf{p}'^T d\mathbf{p}'$, then

$$\tilde{\mathbf{E}} = -\alpha (\mathbf{I} - \hat{\mathbf{k}} \hat{\mathbf{k}}^T) \cdot \int \tilde{\Psi}' \mathbf{p}' \mathbf{p}'^T d\mathbf{p}' \cdot \hat{\mathbf{k}} \hat{\mathbf{k}}^T. \quad (16)$$

Substituting Eqs. (14,16) into Eq. (13), we get a closed equation for the distribution mode $\tilde{\Psi}$

$$\begin{aligned} (\sigma + \lambda_0 + ik \cos \theta) \tilde{\Psi} &= \frac{-3\alpha\gamma}{4\pi} \cos \theta \sin \theta [F_1 + F_2] \\ &+ \frac{\lambda_0}{4\pi} \left[\frac{\chi\beta_2}{(\beta_1 + k^2 D_c)} ik (\cos \theta - \frac{\delta}{3}) + 1 \right] G \\ &+ \frac{\lambda_0}{4\pi} \delta \sin \theta [H_1 + H_2 + H_3] \end{aligned} \quad (17)$$

where w.l.o.g. we let $\hat{\mathbf{k}} = \hat{\mathbf{z}}$ and for simplicity defined

$$\begin{aligned} F_1 &= \cos \phi \int_0^{2\pi} d\phi' \cos \phi' \int_0^\pi d\theta' \sin^2 \theta' \cos \theta' \tilde{\Psi}' \\ F_2 &= \sin \phi \int_0^{2\pi} d\phi' \sin \phi' \int_0^\pi d\theta' \sin^2 \theta' \cos \theta' \tilde{\Psi}' \end{aligned}$$

$$\begin{aligned}
G &= \int_0^{2\pi} d\phi' \int_0^\pi d\theta' \sin \theta' \tilde{\Psi}' \\
H_1 &= \cos \phi \int_0^{2\pi} d\phi' \cos \phi' \int_0^\pi d\theta' \sin^2 \theta' \tilde{\Psi}' \\
H_2 &= \sin \phi \int_0^{2\pi} d\phi' \sin \phi' \int_0^\pi d\theta' \sin^2 \theta' \tilde{\Psi}' \\
H_3 &= \int_0^{2\pi} d\phi' \int_0^\pi d\theta' \sin \theta' \cos \theta' \tilde{\Psi}'. \tag{18}
\end{aligned}$$

Eq. (17) constitutes a linear eigenvalue problem for the perturbation mode $\tilde{\Psi}$ and the growth rate σ . To obtain the eigenvalue relations, we proceed as in¹⁷ and apply (separately) the above operators F_1, H_1, G, H_3 on both sides of the $\tilde{\Psi}$ Eq. (17). The equations relating F_1, H_1, G, H_3 can be written more concisely as

$$\begin{aligned}
F_1 &= \frac{-3\alpha\gamma}{4} J_1 F_1 + \frac{\lambda_0\delta}{4} J_2 H_1 \\
H_1 &= \frac{-3\alpha\gamma}{4} J_2 F_1 + \frac{\lambda_0\delta}{4} J_3 H_1 \\
G &= \frac{\lambda_0}{2} \text{Rik}(1 - \frac{\delta}{3}) J_4 G + \frac{\lambda_0}{2} J_5 G + \frac{\lambda_0\delta}{2} J_4 H_3 \\
H_3 &= \frac{\lambda_0}{2} \text{Rik}(1 - \frac{\delta}{3}) J_6 G + \frac{\lambda_0}{2} J_4 G + \frac{\lambda_0\delta}{2} J_6 H_3
\end{aligned}$$

and the integrals involved are named

$$\begin{aligned}
J_1 &= \int_0^\pi \frac{\sin^3 \theta \cos^2 \theta}{\sigma + \lambda_0 + ik \cos \theta} d\theta \\
&= \frac{2a^3}{ik} - \frac{4a}{3ik} + \frac{(a^4 - a^2)}{ik} \log \left(\frac{a-1}{a+1} \right) \\
J_2 &= \int_0^\pi \frac{\sin^3 \theta \cos \theta}{\sigma + \lambda_0 + ik \cos \theta} d\theta = -J_1/a \\
J_3 &= \int_0^\pi \frac{\sin^3 \theta d\theta}{\sigma + \lambda_0 + ik \cos \theta} = \frac{2a}{ik} + \frac{(a^2 - 1)}{ik} \log \left(\frac{a-1}{a+1} \right) \\
J_4 &= \int_0^\pi \frac{\sin \theta \cos \theta}{\sigma + \lambda_0 + ik \cos \theta} d\theta = \frac{2}{ik} + \frac{a}{ik} \log \left(\frac{a-1}{a+1} \right) \\
J_5 &= \int_0^\pi \frac{\sin \theta \cos \theta}{\sigma + \lambda_0 + ik \cos \theta} d\theta = -\frac{1}{ik} \log \left(\frac{a-1}{a+1} \right) \\
J_6 &= \int_0^\pi \frac{\sin \theta \cos^2 \theta}{\sigma + \lambda_0 + ik \cos \theta} d\theta = -aJ_4.
\end{aligned}$$

For simplicity we have defined $a = (\sigma + \lambda_0)/ik$ and $R = \chi\beta_2/(\beta_1 + k^2 D_c)$. The equations for F_2, H_2 are similar to those for F_1, H_1 .

Note how the equations separate into two groups: F_1, H_1 and G, H_3 . By combining the first two into one equation for F_1 and the last two into one equation for G , we obtain two separate dispersion relations that are compactly written as:

$$0 = \left(1 + \frac{3\alpha\gamma}{4} J_1 \right) \left(1 - \frac{\lambda_0\delta}{4} J_3 \right) - \frac{\lambda_0\delta}{4} J_2 \frac{(-3\alpha\gamma)}{4} J_2 \tag{19}$$

$$\begin{aligned}
0 &= \left(1 - \frac{\lambda_0\delta}{2} J_6 \right) \left(1 - \frac{\lambda_0}{2} \text{Rik}(1 - \frac{\delta}{3}) J_4 - \frac{\lambda_0}{2} J_5 \right) \\
&\quad - \frac{\lambda_0\delta}{4} J_4 \left(\frac{\lambda_0}{2} \text{Rik}(1 - \frac{\delta}{3}) J_6 + \frac{\lambda_0}{2} J_4 \right). \tag{20}
\end{aligned}$$

For isotropic suspensions ($\delta = 0$) these reduce to the two separate relations found by Lushi *et. al.*^{16,17} for auto-chemotactic active suspensions. Here the two relations, while again distinct and arising from the hydrodynamic and chemotactic instabilities respectively, are both affected by the tumble correlations parameter δ .

The tumbling non-isotropy enters *both* Eq. (19) and Eq. (20), which we will name the hydrodynamics and auto-chemotactic dispersion relations respectively. The hydrodynamic relation is also affected by the basic stopping rate λ_0 . The auto-chemotactic relation is unaffected by the hydrodynamics and swimming mechanism, as evidenced by the lack of α or γ parameters in it. The auto-chemotactic relation is of course affected by the chemo-attractant dynamics, as evidenced by the presence of the term $R = \chi\beta_1/(\beta_2 + k^2 D_c)$ which comes from inverting the quasi-static chemo-attractant equation.

B. Long-wave asymptotic expansions

The dispersion relations of Eqs. (19) and (20) cannot be solved exactly for the growth rate σ . To get insight in the behavior of the system, we look for long-wave (small k) asymptotic solutions. Omitting the details of the lengthy calculation, we obtain the following two branches

$$\sigma_{H1} \approx -\lambda_0 + \frac{-\alpha\gamma}{5} + \frac{5}{7\alpha\gamma} \frac{(9\alpha\gamma + 22\lambda_0\delta)}{(3\alpha\gamma + 5\lambda_0\delta)} k^2 + \dots \tag{21}$$

$$\sigma_{H2} \approx -\lambda_0 \left(1 - \frac{\delta}{3} \right) - \frac{3}{5\lambda_0\delta} \frac{(6\alpha\gamma + 5\lambda_0\delta)}{(3\alpha\gamma + 5\lambda_0\delta)} k^2 + \dots \tag{22}$$

From Eq. (21) we can see that there is a long-wave instability arising from the fluid dynamics in pusher swimmer suspensions ($\alpha = -1$) with elongated shape ($\gamma \neq 0$).

The auto-chemotactic relation Eq. (20) gives only one branch at small k that still satisfies the integral relations:

$$\sigma_C \approx \frac{\bar{\chi}\lambda_0(1 - \delta/3) - 1}{3\lambda_0(1 - \delta/3)} k^2 + O(k^3) \tag{23}$$

where we have denoted $\bar{\chi} = \chi\beta_2/\beta_1$.

This asymptotic solutions look similar in form to the ones for isotropic tumbles discussed in^{16,17}. The chemotactic instability in Eq. (23) tells us the anisotropy has a significant impact for a system of finite size. Anisotropic tumbles overall have a stabilizing effect on the suspension, since the growth rate now is smaller due to it being multiplied by $(1 - \delta/3)$, $\delta < 1$ at the highest order of k . Specifically, if all other parameters are kept constant, this tells us that the chemotactic sensitivity χ has to be greater to overcome the tumbling anisotropy.

From Eq. (23), we can obtain a range of parameters for which to obtain $\sigma_C > 0$ and have a chemotactic instability. That happens for $\bar{\chi}\lambda_0(1 - \delta/3) > 1$, or specifically $\chi\beta_2/\beta_1 > 1/[\lambda_0(1 - \delta/3)]$.

The stability analysis of the two-dimensional system is discussed in the Appendix-VIB.

C. Solving the Dispersion Relation

We use an iterative solver to solve numerically the dispersion relations in Eqs. (19, 20) for $\sigma(k)$. To ensure that we do not obtain spurious solutions, we start with the asymptotic expressions in Eqs. (21) and (23) as initial guesses for small k . We then solve for σ_k for each increasing k and use previous k solution as an initial guesses. The numerical solutions are checked that they can still satisfy the integral relations of Eqs. (19,20).

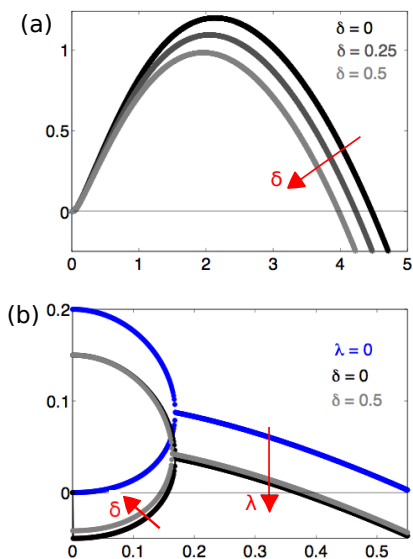


FIG. 1. (color online) (a) Numerical solution for $\sigma_C(k)$ of the auto-chemotactic relation Eq. (20) for $\chi = 20$, $D_c = 1/20$, $\lambda = 0.25$ and a variety of tumbling anisotropy parameters $\delta = 0, 0.25, 0.5$. (b) (a) Numerical solution for $\sigma_H(k)$ of the hydrodynamic relation Eq. (19) for pushers $\alpha = -1$ for $\lambda_0 = 0, 0.05$ and tumbling anisotropy parameters $\delta = 0, 0.5$. Red arrows show the effect of an increasing parameter.

Long-wave asymptotics on the auto-chemotaxis dispersion relation given in Eq. (20) gives that for $(\chi\beta_2/\beta_1)\lambda_0 > (1 - \delta/3)$ there are wavenumbers with $Re(\sigma_C(k)) > 0$, for pushers and pullers alike and any shape parameter γ . Auto-chemotaxis introduces an instability branch, which is solved numerically from Eq.(20) and plotted in Fig.1a. From the plots we see that the tumbling anisotropy δ can have a visible effect on the growth rates, as also expected from the small k analysis. The range of wavenumbers with $Re(\sigma_C(k)) > 0$ is smaller for $\delta > 0$.

The solution to the hydrodynamics relation is shown in Fig.1b for rod-like $\gamma = 1$ for tumbling pusher swimmers $\alpha = -1$ with basic stopping rate $\lambda_0 = 0.05$ and cases $\delta = 0, 0.5$. The branch $\lambda_0 = 0.05$ and $\delta = 0$ is ex-

actly that obtained by Lushi *et al.*^{16,17} for swimmers with uncorrelated tumbles. The addition of a small tumbling anisotropy $\delta = 0.5$ has barely a visible effect on σ_H .

In the case of pullers $\alpha = -1$, there is no hydrodynamic instability as $Re(\sigma_H(k)) < 0$ for any λ_0 and δ .

For non-tumbling pushers ($\alpha < 0$) there is a hydrodynamic instability for a finite band of wavenumbers $k = 0$ until $k_c \approx 0.55$ ^{12,23,24}. Tumbling diminishes this range of unstable wave-numbers since both branches are brought down by λ_0 . As noted in Lushi *et al.*^{16,17}, $\lambda_0 \geq 0.2$ turns off the hydrodynamic instability for any system size, for any swimmer shape γ , and, as can be surmised from the plot in Fig. 1, any tumbling anisotropy parameter δ .

D. Phase Space

Linear theory shows that there is a range of λ_0 for which there is a hydrodynamic instability in pusher suspensions. If $\lambda_0 \geq 0.2$, there is no hydrodynamic instability for any system size and any swimmer shape γ , since, as seen in Fig. 1, $Re(\sigma_H(k)) \leq 0.2$. For an auto-chemotactic instability we need $\chi\beta_2/\beta_1 > 1/[\lambda_0(1 - \delta/3)]$.

This connects the auto-chemotaxis parameters χ , β_1 , β_2 to the basal tumbling rate λ_0 and correlation of tumbles parameter δ . This information about the parameters is assembled in a phase diagram in Fig. 2, which shows the dynamical regimes we expect based on the linear analysis and nonlinear simulations.

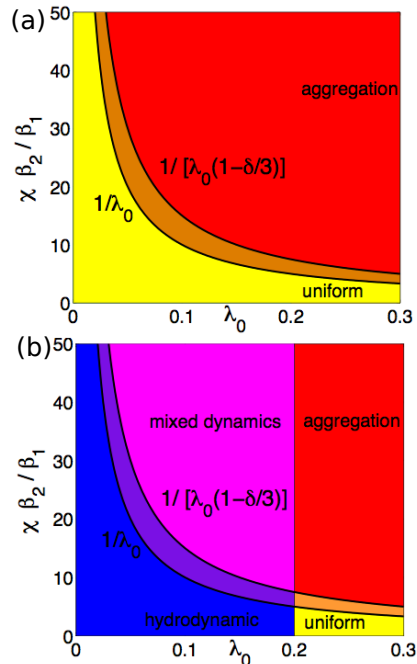


FIG. 2. (Color online) Phase space of various regimes for auto-chemotactic and/or hydrodynamic instabilities in suspensions of (a) pullers or neutral swimmers, (b) pushers as a function of (a) the basal tumbling frequency λ_0 , correlation of tumbles parameter δ and chemotactic parameters χ, β_1, β_2 . The curve $1/[\lambda_0(1 - \delta/3)]$ is shown for $\delta = 0$ and $\delta = 1$. Linear theory predicts an auto-chemotactic instability for the parameter in the space above this curve.

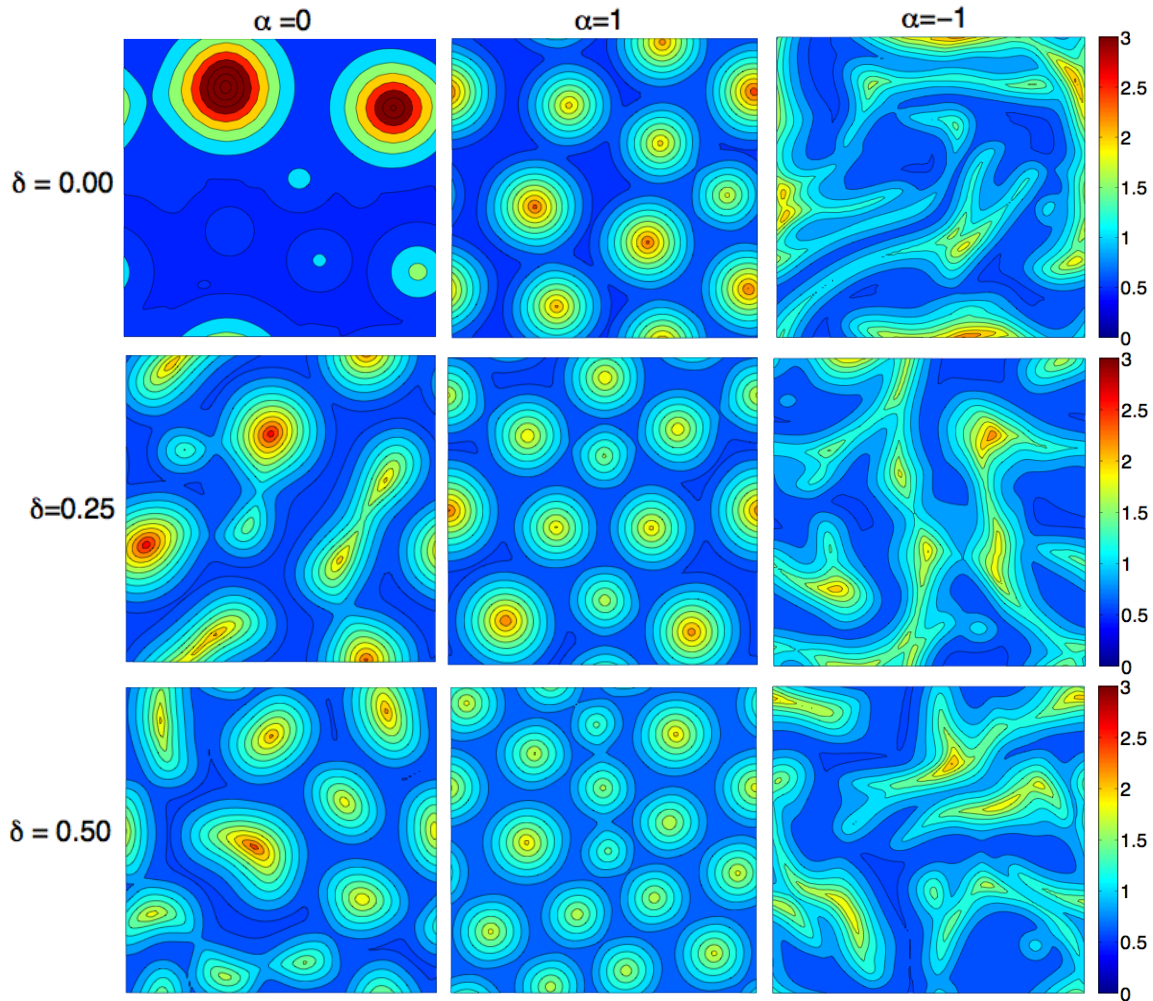


FIG. 3. (Color online) Snapshot of the dynamics of micro-swimmers at long times. Here shown are the cases of “neutral” swimmers ($\alpha = 0$), pullers ($\alpha = +1$) and pushers ($\alpha = -1$) with isotropic tumbling ($\delta = 0$) or with non-zero tumbling direction correlation parameters ($\delta = 0.25, 0.5$).

IV. NONLINEAR SIMULATIONS

We perform flu numerical simulations of the nonlinear system to investigate the dynamics of a variety of motile suspensions under the influence of a swimmer-produced chemo-attractant. In 3D the model involves five configuration variables, three spatial and two angles, which makes the simulations computationally expensive. As in our previous work^{16,17}, we resort to simulations in 2D periodic systems in which the particles are constrained in the (x, y) -plane with swimmer direction parametrized by an angle $\theta \in [0, 2\pi)$ so that the direction is described by $\mathbf{p} = (\cos \theta, \sin \theta, 0)$. The distribution function Ψ then is invariant along the z -direction: $\Psi(\mathbf{x}, \mathbf{p}, t) = \Psi(x, y, \theta, t)$.

Since all the variables are periodic in x, y and θ directions, we can use fast Fourier Transforms to do the all the spatial differentiations and also solve the fluid equations Eq. (7). The integrations in θ to obtain the swimmer density Φ in Eq. (9) and active particle stresses Σ^a in Eq.(8) were done using the trapezoidal rule. Here we typically will use 128 – 256 points in the (x, y) directions

and 32 – 64 in the θ direction.

The conservation equation Eq. (1) and the chemo-attractant equation Eq. (10) are integrated using a second order in time Crank-Nicholson-Adams-Bashforth time-stepping scheme. Particle translational and rotational diffusions as well as chemo-attractant diffusion are included in all the simulations with typical values of $D = d_r = 0.025$ and $D_c = 0.05$, unless otherwise noted. Here we will focus only on elongated rod-shaped swimmers with $\gamma = 1$ and the spatial box 50×50 since linear theory predicts hydrodynamical instability is maximized this choice. The initial condition for the initial swimmer distribution is a uniform isotropic suspension perturbed as

$$\Psi(\mathbf{x}, \theta, 0) = \frac{1}{2\pi} \left[1 + \sum_i \epsilon_i \cos(\mathbf{k}_i \cdot \mathbf{x} + \xi_i) P_i(\theta) \right], \quad (24)$$

with ϵ_i a random small coefficient ($\epsilon_i \in [-0.01, 0.01]$), ξ_i a random phase, and $P_i(\theta)$ a third order polynomial of $\sin \theta$ and $\cos \theta$ with random coefficients.

A. Dynamics: Qualitative Comparisons

We look at the nonlinear dynamics of the system for all the types of swimmers (neutral with $\alpha = 0$, pullers with $\alpha = +1$ and pushers with $\alpha = -1$), when there is no tumbling anisotropy ($\delta = 0$) and two cases when there is a slight tumbling anisotropy ($\delta = 0.25$ and $\delta = 0.5$). We pick chemotactic parameters $\chi = 20, \beta_1 = \beta_2 = 1/4$ and basal tumbling $\lambda_0 = 0.5$ that lie in the aggregation regime of all types of swimmers in the phase spaces shown earlier in Fig. 2.

As explored in our previous studies^{16,17}, isotropic suspensions ($\delta = 0$) of neutral, puller and pusher swimmers differ in their pattern morphology. For neutral swimmers ($\alpha = 0$) where the fluid flows are not taken into account, the observed dynamics is that of continuous aggregation into large peaks. For puller swimmers ($\alpha = +1$), aggregation into stable peaks also occurs, but these peaks are smaller and circular due to the generated straining fluid flows that keep them from merging further^{16,17}. For pushers ($\alpha = -1$) we observe dynamic aggregation of the swimmers into irregular peaks that continuously move, merge and break apart. This effect is due to the collectively-generated fluid flows that are known to occur even in the absence of chemotaxis²⁴, but here these flows are able to transport the chemo-attractant field as well as the swimmers themselves and thus can affect the collective chemotactic dynamics^{16,17}.

The anisotropy in the tumbling directions has an interesting effect in the swimmers' collective chemotactic dynamics. Linear stability predicts that increasing tumbling correlation parameter δ will dampen the chemotactic instability, but have no visible impact in the hydrodynamic instability, as seen from asymptotic results Eqs. (21, 23) and illustrated in Fig. 1. The main dynamics is still determined by the type of swimmer (neutral, puller, pusher), however some differences are clearly visible. Most notably, the tumbling anisotropy has affected the number of the resulting aggregation peaks. For example, for isotropic suspensions ($\delta = 0$), the neutral swimmer suspension shown in the example of Fig. 3 has ≈ 2 peaks and the puller suspension has ≈ 9 peaks. With slight tumbling anisotropy ($\delta = 0.25$), the number of peaks in the neutral swimmer suspension has increased to ≈ 6 and in the puller to ≈ 11 . With higher tumbling anisotropy ($\delta = 0.5$), the number of peaks increases even further to ≈ 10 in the neutral swimmer case and ≈ 16 peaks in the puller swimmer case.

Curiously, the pusher suspension in Fig. 3 does not seem to be visibly affected when the tumbling anisotropy parameter δ is increased. The collective dynamics of the pusher swimmers is still typified by dynamic aggregation into peaks that continuously merge, move, and then break apart. The height of these peaks is not visibly affected much.

B. Dynamics: Quantitative Comparisons

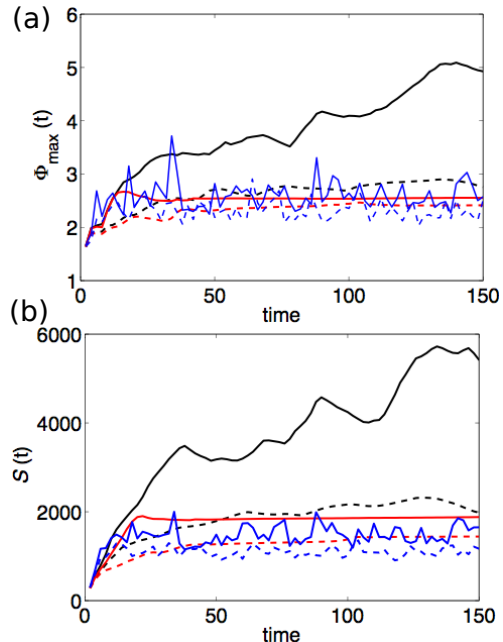


FIG. 4. (Color online) Evolution of the maximum of the swimmer concentration Φ and the system configurational entropy $S(t)$ in time. The cases shown are for neutral (black line), puller (red line) and pusher swimmers (blue line) for isotropic suspensions (solid lines) and anisotropic suspensions with $\delta = 0.25$ (dashed lines).

To quantify the effect of the tumbling anisotropy in the various suspensions, we track the evolution in time of the swimmer concentration maximum Φ_{max} and the configurational entropy

$$S(\mathbf{x}, \mathbf{p}) = \int \int \Psi(\mathbf{x}, \mathbf{p}) \log(\Psi(\mathbf{x}, \mathbf{p})) d\mathbf{p} d\mathbf{x} \quad (25)$$

which plays the role of a system energy here²⁴.

The results, shown in Fig. 4, show that while the tumbling anisotropy does indeed have a dampening effect on the swimmer suspension dynamics which may not be visible in all the snapshots of the dynamics in Fig. 3. The maximum concentration for anisotropic suspensions, be that of neutral, pusher or puller swimmers, is lower than in the isotropic suspension cases with otherwise the same parameters and initial conditions. Indeed, even in the pusher case, the maximum swimmer concentration is over time lower in the anisotropic suspension.

The configurational entropy tells us the same story: the tumbling anisotropy dampens the dynamics in all the swimmer suspensions as the lines for the anisotropic cases are lower than the isotropic cases over long times. The major differences in the dynamics still arise due to the swimmer type.

Qualitatively similar results were obtained for other basal tumbling λ_0 and chemotactic parameters χ tried.

V. DISCUSSION AND CONCLUSION

It is well-known that bacteria, after which the so-called pusher swimmers are modeled, perform a run-and-tumble motion even in the absence of chemotaxis^{4,5}, and in some fashion so do micro-algae like *Chlamydomonas reinhardtii*, after which the puller swimmers are modeled²². To move up a chemo-attractant gradient, bacteria are known to modify their tumbling rate in response to the local attractant concentration¹⁸ and bacteria like *Escherichia coli* are known to aggregate in complex and intricate patterns^{6,19}. These experiments have inspired many theoretical and computational studies of chemotaxis in particular^{13,14,25,26,30} and micro-swimmer dynamics in general^{3,11,21}. However, it is also known that the tumbles in bacteria like *Escherichia coli* are not completely random since the pre- and post-tumble directions are slightly correlated^{25,28,29}. The effect of such anisotropy in the chemotactic run-and-tumble motion and collective dynamics has barely been explored^{28,29}.

We have investigated analytically and computationally the role of correlated tumbles in various micro-swimmer suspensions. We considered the dynamics resulting from the full coupling of the anisotropic run-and-tumble chemotaxis to the motion of the immersing fluid and the chemo-attractant that the swimmers themselves produce. The types of swimmers considered here are pushers (like swimming bacteria) and pullers (like micro-algae) that are known to individually and collectively disturb the surrounding fluid and affect the neighbors' motion^{8,10,23,27-29}, and theoretical neutral swimmers that do not create any fluid disturbances. While neutral and puller swimmers are known to accumulate in peaks due to auto-chemotaxis, pushers dynamically aggregate into peaks as a result of the collectively generated fluid flows^{16,17}.

Linear analysis revealed that the correlated tumbling affects chemotactic aggregation in all types of swimmers alike and has a stabilizing effect. An instability due to hydrodynamics occurs only in pusher swimmers, and linear analysis predicted that the effect of the correlated tumbles in that case is minor. However, simulations of the full coupled system showed subtle but non-trivial effects of the tumbling anisotropy in the pattern formation. The tumbling anisotropy is predictably a stabilizer on the chemotactic growth of the aggregates in all types of swimmer suspensions. Unpredicted by linear analysis, the tumbling anisotropy is most visibly manifested in the increased number of stable aggregate peaks in suspensions of neutral and puller swimmers. The aggregates observed in the long-time dynamics of the anisotropically-tumbling swimmer suspensions are on average not as high as in the isotropically-tumbling swimmer suspensions.

We explored analytically and computationally the effect of anisotropic tumbles, as known to occur in motion of *E. coli*, in the dynamics of various motile suspensions. We hope it leads to an increased interest in studies of chemotactic swimmers and other active particles.

ACKNOWLEDGEMENTS

The author thanks Raymond Goldstein, Christel Hohenegger and Michael Shelley for helpful discussions.

- ¹W. Alt. Biased random walk models for chemotaxis and related diffusion. approximations. *J. Math. Bio.*, **9**, 147, (1980).
- ²B.L. Bassler. Small talk. Cell-to-cell communication in bacteria. *Cell* **109**, 421 (2002).
- ³R.N. Bearon and T.J. Pedley. Modelling run-and-tumble chemotaxis in a shear flow. *Bull. Math. Bio.*, **62**, 775 (2000).
- ⁴H.C. Berg. *Random Walks in Biology. Expanded Ed.* Princeton University Press (1993).
- ⁵H.C. Berg and D.A. Brown. Chemotaxis in *Escherichia Coli* analyzed by three-dimensional tracking. *Nature*, **239**, 500 (1972).
- ⁶E.O. Budrene and H.C. Berg. Complex patterns formed by motile cells of *Escherichia coli*. *Nature* **349**, 630 (1991).
- ⁷K.C. Chen, R.M. Ford, and P.T. Cummings. Cell balance equation for chemotactic bacteria with a biphasic tumbling frequency. *J. Math. Bio.*, **47**, 518 (2003).
- ⁸L. Cisneros, R. Cortez, C. Dombrowski, R.E. Goldstein, and J.O. Kessler. Fluid dynamics of self-propelled microorganisms, from individuals to concentrated populations. *Exp. Fluids*, **43**, 737 (2007).
- ⁹L.H. Cisneros, J.O. Kessler, S. Ganguly, and R.E. Goldstein. Dynamics of swimming bacteria: Transition to directional order at high concentration. *Phys. Rev. E*, **83**, 061907 (2011).
- ¹⁰C. Dombrowski, L. Cisneros, S. Chatkaew, R. E. Goldstein, and J. O. Kessler. Self-concentration and large-scale coherence in bacterial dynamics. *Phys. Rev. Lett.*, **93**, 098103 (2004).
- ¹¹N.A. Hill and T.J. Pedley. Bioconvection. *Fluid Dyn. Res.*, **37**, 1 (2005).
- ¹²C. Hohenegger and M.J. Shelley. On the stability of active suspensions. *Phys. Rev. E*, **81**, 046311 (2010).
- ¹³E.F. Keller and L.A. Segel. Initiation of slime mold aggregation viewed as an instability. *J. Theor. Biol.*, **26**, 399 (1970).
- ¹⁴E.F. Keller and L.A. Segel. Model for chemotaxis. *J. Theor. Biol.*, **30**, 225 (1971).
- ¹⁵E. Lushi. Chemotaxis and other effects in active particle suspensions. *Ph.D. dissertation*, New York University, (2011).
- ¹⁶E. Lushi, R.E. Goldstein and M.J. Shelley. Collective chemotactic dynamics in the presence of self-generated fluid flows. *Phys. Rev. E*, **86**, 040902(R), (2012).
- ¹⁷E. Lushi, R.E. Goldstein and M.J. Shelley. Auto-chemotactic active suspensions: modeling, analysis and simulations. arXiv preprint arXiv:1310.7614 (2013).
- ¹⁸R.M. Macnab and D.E. Koshland. The gradient-sensing mechanism in bacterial chemotaxis. *Proc. Natl. Acad. Sci. USA*, **69**, 2509 (1972).
- ¹⁹N. Mittal, E.O. Budrene, M.P. Brenner and A. van Oudenaarden. Motility of *Escherichia Coli* cells in clusters formed by chemotaxis. *Proc. Natl. Acad. Sci. USA*, **100**, 13259 (2003).
- ²⁰S. Park, P.M. Wolanin, E.A. Yuzbashyan, P. Silberzan, J.B. Stock, and R.H. Austin, Motion to form a quorum. *Science*, **301**, 188 (2003).
- ²¹T.J. Pedley and J.O. Kessler. Hydrodynamic phenomena in suspensions of swimming microorganisms. *Annu. Rev. Fluid Mech.*, **24**, 313 (1992).
- ²²M. Polin, I. Tuval, K. Drescher, J.P. Gollub, R.E. Goldstein. *Chlamydomonas* swims with two gears in a eukaryotic version of run-and-tumble locomotion. *Science* **325** (5939) 487-490 (2009).
- ²³D. Saintillan and M.J. Shelley. Instabilities and pattern formation in active particle suspensions: Kinetic theory and continuum simulations. *Phys. Rev. Lett.*, **100**, 178103 (2008).
- ²⁴D. Saintillan and M.J. Shelley. Instabilities, pattern formation, and mixing in active suspensions. *Phys. Fluids*, **20**, 123304 (2008).

- ²⁵M.J. Schnitzer. Theory of continuum random walks and application to chemotaxis. *Phys. Rev. E*, **48**, 2553 (1993).
- ²⁶M.J. Schnitzer, S.M. Block, H.C. Berg, and E.M. Purcell. Strategies for chemotaxis. *Symp. Soc. Gen. Microbiol.*, **46**, 15 (1990).
- ²⁷A. Sokolov, R.E. Goldstein, F.I. Feldstein and I.S. Aranson. Enhanced mixing and spatial instability in concentrated bacteria suspensions. *Phys. Rev. E*, **80**, 031903 (2009).
- ²⁸G. Subramanian and D.L. Koch. Critical bacterial concentration for the onset of collective swimming. *J. Fluid Mech.*, **632**, 359 (2009).
- ²⁹G. Subramanian and D.L. Koch. Collective hydrodynamics of swimming microorganisms: Living fluids. *Ann. Rev. Fluid Mech.* **43** 637-659 (2011).
- ³⁰M.J. Tindall, P.K. Maini, S.L. Porter, and J.P. Armitage. Overview of mathematical approaches used to model bacterial chemotaxis ii: bacterial populations. *Bull. Math. Bio.*, **70**, 1570 (2008).

VI. APPENDIX

A. The model in two dimensions

We briefly mention here how the equations in two dimensions differ from the three-dimensional ones. In two dimensions we have only one orientation angle $\theta \in [0, 2\pi]$ with $\mathbf{p} = (\cos \theta, \sin \theta)$, and the differences from the Run-and-Tumble 3D system Eqs. (1, 7, 10) are only in the following equations

$$\begin{aligned} \frac{\partial \Psi}{\partial t} &= -\nabla_x \cdot (\Psi \dot{\mathbf{x}}) - \partial_\theta (\Psi \dot{\theta}) \\ &+ \left[\Psi \lambda(\mathbf{p}) - \int_0^{2\pi} \mathbf{K}(\mathbf{p}, \mathbf{p}'; \delta) \Psi' \lambda(\mathbf{p}') d\theta \right] \\ \dot{\theta} &= \mathbf{p}_\perp \cdot (\gamma \mathbf{E} + \mathbf{W}) \mathbf{p} - d_r \partial_\theta (\ln \Psi) \\ \Sigma^a &= \alpha \int_0^{2\pi} \Psi(\mathbf{x}, \theta, t) (\mathbf{p} \mathbf{p} - \mathbf{I}/2) d\theta \end{aligned} \quad (26)$$

where $\mathbf{p}_\perp = (-\sin \theta, \cos \theta)$ is the unit vector perpendicular to the particle orientation. In 2D the isotropic suspension state is given by $\Psi_0 = 1/2\pi$.

The two-dimensional Run-and-Tumble model does not differ much in appearance from the three-dimensional one in Eq.(1), except that the turning kernel that satisfies all the needed conditions in two-dimensions is given by

$$\mathbf{K}(\mathbf{p}, \mathbf{p}'; \delta) = \frac{1}{2\pi I_0(\delta)} e^{\delta \mathbf{p} \cdot \mathbf{p}'}. \quad (27)$$

Here $I_0(\delta)$ is a Modified Bessel function of the First Kind.

B. Linear Stability in 2D

As with the 3D system in Section III, we consider quasi-static chemo-attractant dynamics Eq. (11) and linearized stopping or tumbling rate Eq. (12). Again, we consider plane-wave perturbations of the distribution and chemo-attractant concentration functions about the uniform isotropic state in 2D ($\Psi_0 = 1/2\pi$) and steady-state ($\bar{C} = \beta_2/\beta_1$) respectively. Going through the same procedure outlined in Section III-A, we can obtain a close equation for the distribution mode $\tilde{\Psi}$.

Similarly to 3D, two dispersion relations can be obtained, one related to hydrodynamics due to the appearance of parameters α, γ in it, and the other related to run-and-tumble chemotaxis due to the appearance of parameters $\lambda_0, \chi, \beta_1, \beta_2, D_c$ in it.

The long-wave (small k) asymptotic analysis of these yields the following growth rates from the hydrodynamic and the auto-chemotactic dispersion relations

$$\sigma_{H1} \approx -\lambda_0 - \alpha\gamma/4 + O(k^2) \quad (28)$$

$$\sigma_{H2} \approx -\lambda_0(1 - \delta/2) - O(k^2) \quad (29)$$

$$\sigma_C \approx \frac{\bar{\chi}\lambda_0(1 - \delta/2) - 1}{2\lambda_0(1 - \delta/2)} k^2 + O(k^3) \quad (30)$$

which look qualitatively very similar to the three dimensional ones in Eqs. (21, 23).

As now expected, there are two branches for the growth rate for the hydrodynamic dispersion relation. From Eq. (28) we can see that there is a hydrodynamic instability only for pusher swimmers ($\alpha = -1$) with elongated shape $\gamma \neq 0$. The tumbling anisotropy does not appear in the highest order terms of the dominant branch σ_{H1} . Although the tumbling anisotropy appears in the lesser branch σ_{H2} , this branch stays negative, as also seen in the numerical solution of the 3D analogue in Fig. 1, and has minor effects in the dynamics as shown with the non-linear simulations in Section IV.

Eq. (30) shows that there is an auto-chemotactic instability for all types of swimmer (neutral, puller and pusher) if the involved parameters satisfy the condition $\chi\beta_2/\beta_1 > 1/\lambda_0(1 - \delta/2)$ which is very similar to its three-dimensional analogue.